



Improving the thermocline calculation over the global ocean

Emmanuel Romero¹, Leonardo Tenorio-Fernandez², Esther Portela^{3,4}, Jorge Montes-Aréchiga⁵, and Laura Sánchez-Velasco¹

¹Instituto Politécnico Nacional–Centro Interdisciplinario de Ciencias Marinas (IPN-CICIMAR), Departamento de Oceanología, Av. IPN s/n, La Paz, B.C.S., 23096, México

²CONACyT-Instituto Politécnico Nacional-Centro Interdisciplinario de Ciencias Marinas (IPN-CICIMAR), Av. IPN s/n, La Paz, B.C.S., 23096, México

³Institute for Marine and Antarctic Studies, University of Tasmania, Hobart 7001, Australia

⁴Univ. Brest, Laboratoire d’Océanographie Physique et Spatiale, CNRS, IRD, Ifremer, Plouzané, France

⁵Universidad de Guadalajara, Departamento de Física, Gral. Marcelino García Barragán 1421, Olímpica, 44430 Guadalajara, Jal, México

Correspondence: Leonardo Tenorio-Fernandez (ltenoriof@ipn.mx)

Abstract. According to the typical thermal structure of the ocean, the water column can be divided into three layers: the mixing layer, the thermocline and the deep layer. In this study, we provide a new methodology, based on a function adjustment on the temperature profile, to locate the minimum and maximum depths of the thermocline, and therefore its thickness, to separate the water column into layers. We first validated our methodology by comparing the mixed layer depth obtained with the method proposed here with that of two previous studies. Since we found a very good agreement between the three methods we used the function adjustment to compute the monthly climatologies of the mixed layer depth, the maximum depth of the thermocline and the thermocline thickness, throughout the ocean. We also provide an assessment of the regions of the ocean where our adjustment is valid, and consequently the regions where the thermal structure of the ocean follows the three-layer structure. However, there are ocean regions where the water column cannot be separated into three layers due to the dynamic processes that alter it and the major contribution of salinity to stratification. This assessment highlights the limitations of the existing methods to accurately determine the mixed layer depth and the thermocline in oceanic regions that are particularly turbulent as the Southern Ocean and the northern North Atlantic, among others. The method proposed here has shown to be robust and easy to apply, and it can be used in both local and global studies.

1 Introduction

In most of the ocean, a typical profile of temperature over depth shows maximum temperature at the surface, due to solar radiation, and can be divided into three main layers according to the thermal structure of the ocean: (i) the mixed layer, where the turbulence generated by atmospheric processes homogenizes the temperature and distributes heat throughout the layer; (ii) the thermocline, the layer with the strongest stratification, that separates the upper mixed layer from the deep layer of the ocean; and (iii) the deep layer, where the temperature is practically invariant over time and relatively constant from the lower thermocline to the seafloor. This three-layer structure is similar to the fundamental vertical structure of the world ocean (Sallée et al., 2021), where the central layer is the pycnocline. In most of the ocean, the temperature exerts the main control on the



density of the water column. The exceptions are the polar regions where temperature is very low, and the seawater density is mostly determined by salinity (de Boyer Montégut et al., 2004; Yamaguchi and Suga, 2019; Sallée et al., 2021).

The thermocline is the ocean layer where the temperature changes sharply with depth relative to the upper and lower layers (Fiedler, 2010). Consequently, the thermocline depth is often defined as the depth of the maximum vertical temperature gradient. The characteristics and depths of this layer vary latitudinally and longitudinally (coast-ocean gradients). At low latitudes, the relatively higher temperatures in the upper water column result in strongly stratified thermoclines. In contrast, at high latitudes, where there is generally little difference between the surface and deep layer temperature, the thermocline is weak (Webb, 2021). The strengthening of the upper thermocline in mid-latitudes during summer, when heat flux at the surface is positive and wind mixing is low, is known as the “seasonal thermocline” (Sprintall and Cronin, 2001). In contrast, in tropical and polar regions the seasonal changes are weak. Due to cooling, wind-driven mixing, and a well-stratified thermocline, the mixed layer is deeper in winter (Sprintall and Cronin, 2001).

The mixed layer depth (MLD), which is also the top of the thermocline, thermocline depth, and thermocline strength (Fiedler, 2010) play a key role in determining the vertical distribution of physical and ecological parameters. The thermocline is a physical gradient that plays a key role in climate variability and ocean-atmosphere interactions (Chu and Fan, 2019). The thermocline strength affects buoyancy, heat budgets, circulation, and exchange of properties. Its depth is associated with the habitat and abundance of zooplankton organisms (Southward and Barrett, 1983; Ruvalcaba-Aroche et al., 2022) and is also an ecological boundary for the pelagic organism because strong temperature changes can set habitat distributions and because it often corresponds to gradients in nutrients, oxygen, or other limiting factors. The thermocline thickness also affects the intensity of the primary production. Particularly at the poles, where the thermocline is weaker, enhanced mixing distributes nutrients throughout the water column. In contrast, in equatorial and tropical regions, the strong thermocline prevents nutrient-rich water from the deep layer from reaching the surface (Webb, 2021). Observations of tracer concentrations and model simulations suggest a connection between the equatorial thermocline and mid-latitude ventilation regions (Harper, 2000).

The strength of the ocean stratification has strong implications for the ventilation of the interior ocean and the injection of traces as oxygen and carbon (Sallée et al., 2012; Portela et al., 2020). Therefore, the knowledge and monitoring of the depth and strength of the thermocline is particularly relevant in the context of ocean warming and its effects in the pelagic ecosystem. Recent global studies have found an overall increase of the global ocean stratification (Li et al., 2020) as well as important regional variability in the global pycnocline trend over the past decades (Sallée et al., 2021). For instance, the thickness of the equatorial and tropical thermocline is enhanced under ocean warming, because the surface layer warms more and faster than the lower layers (Yang and Wang, 2009).

Previous regional studies have identified a shallowing and strengthening of the thermocline in the western Pacific Ocean (Vecchi and Soden, 2007) and in the equatorial Pacific (Zelle et al., 2004). Additionally, modeling studies have suggested that important changes in the Pacific Ocean, such as rising sea levels and temperatures, affect the structure of the thermocline from the subtropics to the tropics (Landerer et al., 2007; Overland and Wang, 2007). These changes in thermocline in the western tropical Pacific are considered to influence the properties of ENSO (Luo et al., 2009), which has strong climatic and socio-economical consequences at basin scale, because the organisms change their distribution and abundance.



Different methodologies have been proposed to locate the maximum depth of the mixed layer (e.g., de Boyer Montégut et al., 2004; Holte and Talley, 2009) and the strength and trends of the ocean stratification (Yamaguchi and Suga, 2019; Li et al., 2020; Sallée et al., 2021). However, little efforts have been dedicated to identify and map the MTD on a global scale.

60 This depth can be delimited empirically by locating the rapid temperature change in the profile, other studies are based in, for instance, calculating the thermocline gradient using the exponential leap-forward gradient method (Chu and Fan, 2017), the maximum curvature point method (Jiang et al., 2016), or using a matrix to calculate the temperature strength of each point and filtering those points that meet the thermocline standard ($> 0.2^{\circ}\text{C}/\text{m}$) (Jiang et al., 2017). Additionally, Fiedler (2010) has compared different methods to estimate the mixed layer depth, thermocline depth, and thermocline strength. In his study,

65 the method that gave the best results was the Variable Representative Isotherm (VRI). This method locates the thermocline from the base of the mixed layer to the depth at which temperature has dropped halfway toward the deep-water temperature at 400 m (Fiedler, 2010). Despite few studies applying the above methods to particular regions of the ocean, to the best of our knowledge, there are no studies addressing the MTD on a global scale. The methodologies mentioned above to locate the MLD use the data from the profilers of the Argo program. Argo is an international program that measures the ocean water column

70 using a fleet of autonomous profilers, which are capable of measuring pressure, temperature, salinity, and biogeochemical parameters (Argo, 2022a). These profilers move along ocean currents and measure the water column by making profiles from a depth of two kilometers to the surface.

This paper proposes a simple and efficient methodology to locate the minimum and maximum depth of the thermocline and its thickness, making an adjustment of the sigmoid function to the temperature profiles. Locating these depths helps to conduct

75 research on thermocline-related ocean warming and through the proposed methodology, it will be possible to conduct local and global studies on changes in ocean thermal structure through time and space.

2 Data collection

For all the diagnostics carried out in this study we used the Argo dataset. We downloaded the snapshot of January 2022 (Argo, 2022b) and we used the profiles already evaluated by the delayed mode quality control (DMQC) from January 1998 to

80 December 2021 (more than two million).

We selected pressure, temperature and salinity profiles from the core Argo floats, which typically sample down to 2000 m. We then transformed the in-situ temperature and practical salinity into conservative temperature (Θ), and absolute salinity (S_A), using the definition of the Thermodynamic Equation of SeaWater 2010 (TEOS-10) (McDougall and Barker, 2011).

3 Methodology

85 Previous studies (e.g., de Boyer Montégut et al., 2004; Holte and Talley, 2009) have proposed different methodologies to calculate the MLD on a global scale. Despite the existence of methods to calculate MTD (such as those compared in the revision study of Fiedler (2010)), these have been evaluated with a limited amount of data, and in relatively small tropical and



subtropical areas, therefore excluding profiles of high latitudes. Here we propose to use a new method based on the sigmoid function adjustment in the temperature profile to localize the MTD. Our method takes advantage of the characteristics that this function shares with the typical temperature profiles in most of the ocean: a straight line that represents the homogeneity of the MLD, a diagonal that represents the rapid increase or decrease in temperature with depth (changing the sign of the function) in the thermocline, and a straight line that represents the little variability of the temperature of the deep ocean (Figure 1a).

To locate the MTD, we first computed the vertical maximum of the buoyancy frequency squared (N^2), to locate the most stratified point of the water column. At this point, where the density gradient is the strongest, we consider that it is inside the pycnocline (McDougall and Barker, 2011), and since density is mainly determined by temperature (except at high latitudes), we assume that this point is also inside the thermocline (Fiedler, 2010). Schematically, most of the temperature profiles in all latitudes have a shape similar to the sigmoid function (Equation 1).

$$f(x) = \frac{1}{1 + e^{-x}} \quad (1)$$

To perform the function adjustment, we first locate the most stratified point in the center of the sigmoid function. To this end, we take the temperature profile from the surface to the depth of the most stratified point multiplied by two, in this way, we reduce the maximum depth with which we will work. This is needed to place the sigmoid function, which is symmetrical, in the center of the pycnocline, and fully represent the mixed layer with a straight line. Then we evaluate the direction of the vertical temperature change. If the temperature decreases with depth, the sigmoid function is inverted by multiplying it by -1 , then we normalize the temperature data between 0 and 1 to make the non-linear adjustment of the function. We assess the goodness of the fit with the coefficient of determination (R^2), this coefficient informs on how well the adjusted function approximates the real data, being 1 the best adjustment.

Once the sigmoid has been fitted to the temperature profile, we can determine the MLD and MTD by scrolling through the function. The temperature at a depth of 10 m resulting from the adjustment of the function is taken as a reference and is denormalized, that is, it is transformed again to be represented as a function of depth. The MLD is then determined as the depth where the potential temperature is 0.2°C higher (or lower) than the reference temperature at 10 m (de Boyer Montégut et al., 2004). To locate the MTD, we used the same procedure but going upwards in the function, in this case we take the reference temperature where the deep layer should be located and we look for the difference of 0.2°C by decreasing the depth through the function. Because the method is based on a single nonlinear function adjustment, we can have a precision of even centimeters. The procedure explained above can be seen in Figure 1a and can be used through the script developed (Romero et al., 2022).

This methodology was applied to each of the DMQC Argo profiles. Before we apply our method to locate the MTD, we have validated it by comparing our results for the MLD with other existing methods. To do so, the MLD of each profile of the data set was calculated in three different ways: (i) with the proposed method, (ii) following the methodology of Holte and Talley (2009) and (iii) with the methodology of de Boyer Montégut et al. (2004) (hereinafter, we will refer to the former two methods as HT03 and B04 respectively). HT03 separately calculate the MLD for temperature, salinity and density and choose the highest MLD value, while B04 use a threshold of 0.03kgm^{-3} in the density profile to locate the MLD. To compare the three

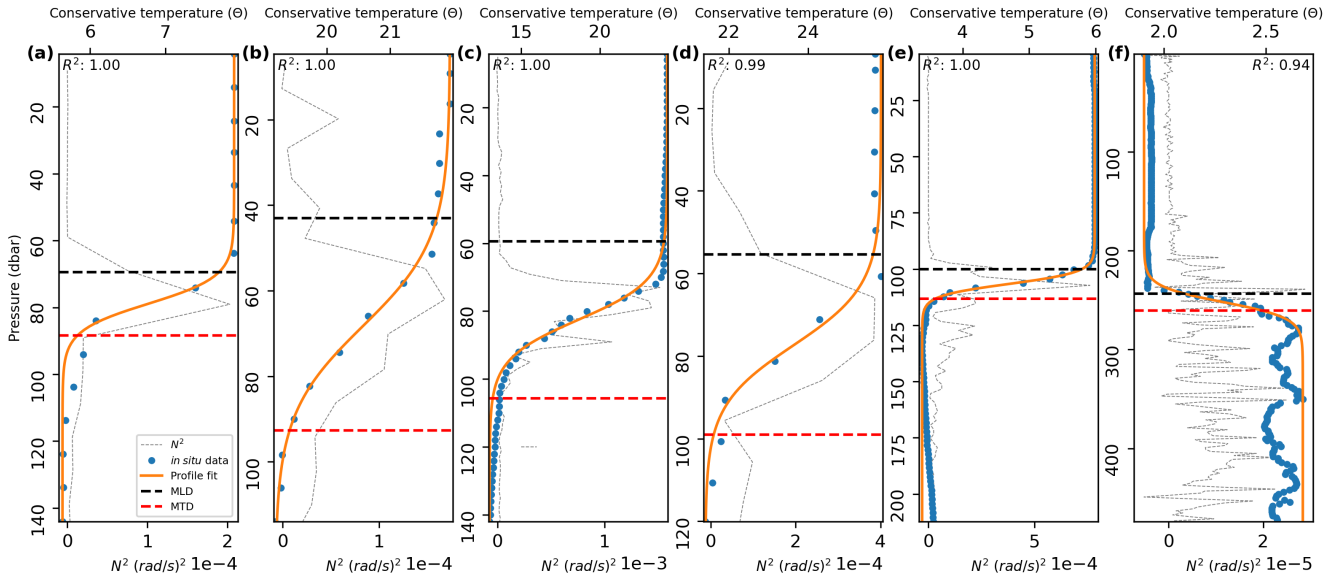


Figure 1. Location of the MTD and the MLD in temperature profiles. (a) 52.95°S and 90.05°W on 01/23/2003. (b) 25.14°S and 93.48°W on 01/12/2013. (c) 1.90°S and 126.07°W on 05/25/2013. (d) 20.02°N and 41.15°W on 12/15/2015. (e) 49.00°N and 174.70°W on 12/13/2017. (f) 60.00°S and 116.86°W on 08/12/2015.

methods to compute de MLD, the ocean was divided in regions following the reference of the Working Group I contribution to the Sixth Assessment Report (AR6-WGI) (Iturbide et al., 2020) of the Intergovernmental Panel on Climate Change (IPCC) and the regional monthly average of the MLD was calculated. Regions with less than 10 averaged values were not taken into account.

125 To carry out our computations we averaged all profiles available for each climatological month in $2^\circ \times 2^\circ$ cells. The choice of the $2^\circ \times 2^\circ$ cells responds to a compromise between keeping reasonable resolution and enough data in each cell for each climatological month. With these data, we then obtained climatologies of the MLD produced by each methodology described above including the one proposed here. Additionally, we provide the monthly average of R^2 in the same grid as a proxy to know the regions of the ocean where the proposed methodology is reliable. We also computed the relative contribution of
 130 temperature (N_T^2) and salinity (N_S^2) to the stratification (N^2) at the most stratified point of the water column, to know the regions where the calculation of the thermocline should also coincide with that of the pycnocline.

4 Results

In order to evaluate the adequacy of the sigmoid function fit, we made a first visual exploration of the temperature profiles in different latitudes of the ocean. Figure 1 shows six temperature profiles with different characteristics, where the MTD and the
 135 MLD computed with the method proposed here are indicated.

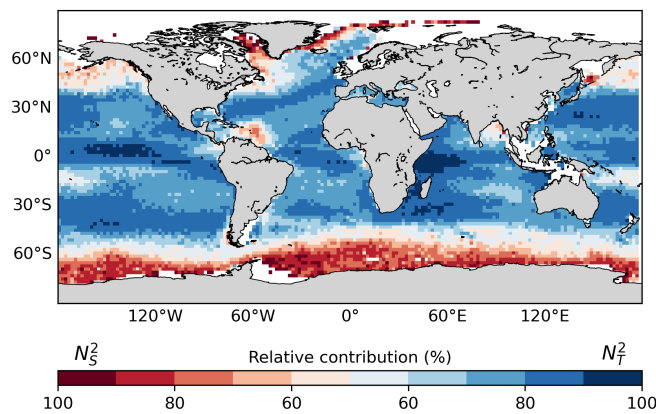


Figure 2. Averaged relative contribution of temperature and salinity at the most stratified point of the ocean water column.

The temperature profiles shown in Figure 1a, b and f were taken in the northern hemisphere, the profile in Figure 1c in the equator and the profiles in Figure 1d and e in the southern hemisphere. In the profiles from Figure 1a-e the temperature drops in the thermocline as the depth increases, while the profile from Figure 1f shows temperature increase with depth. Profiles in Figure 1e and f show greater variability in their stratification, Figure 1f shows that despite the high variability in the deep layer, the methodology correctly determines the MLD and MTD. In all cases R^2 approaches to 1. Both, the visual examination and the values of R^2 , indicate that our methodology correctly locates the MTD and the MLD at different latitudes.

4.1 Validation of the method: MLD calculation

To make the adjustment of the sigmoid function, the most stratified point of the water column is used as the central point of the adjustment. Figure 2 illustrates the regions of the ocean where salinity (red colors) or temperature (blue colors) dominate the stratification. This has to be taken into account when interpreting the results of our adjustment, which bases on the temperature as the main control on density and stratification. Although the N^2 computation is based on density, the stratification of the most stratified point of the water column of most of the ocean is dominated by the temperature, while salinity dominates south of 60°S, north of 45°N in the Pacific Ocean, in the Labrador Sea and north of 60°N in the Atlantic Ocean. Salinity also dominates the stratification in very localized regions of the tropical ocean such as the Caribbean Sea and the Bay of Bengal, due to freshwater supply from river runoff, precipitation (Gévaudan et al., 2021), strong rainfall and major river discharge (Li et al., 2017). In these salinity-dominated regions, the water column does not follow the typical thermal three-layer structure, so our method is not optimal.

In addition to identifying the regions where our method should be applied with caution due to the minor role of temperature in setting the stratification of the water column, we provide another proxy of the goodness of our adjustment. To illustrate the accuracy of our method, to fit the sigmoid function to temperature profiles, we provide a map of the monthly average of R^2 (Figure 3).

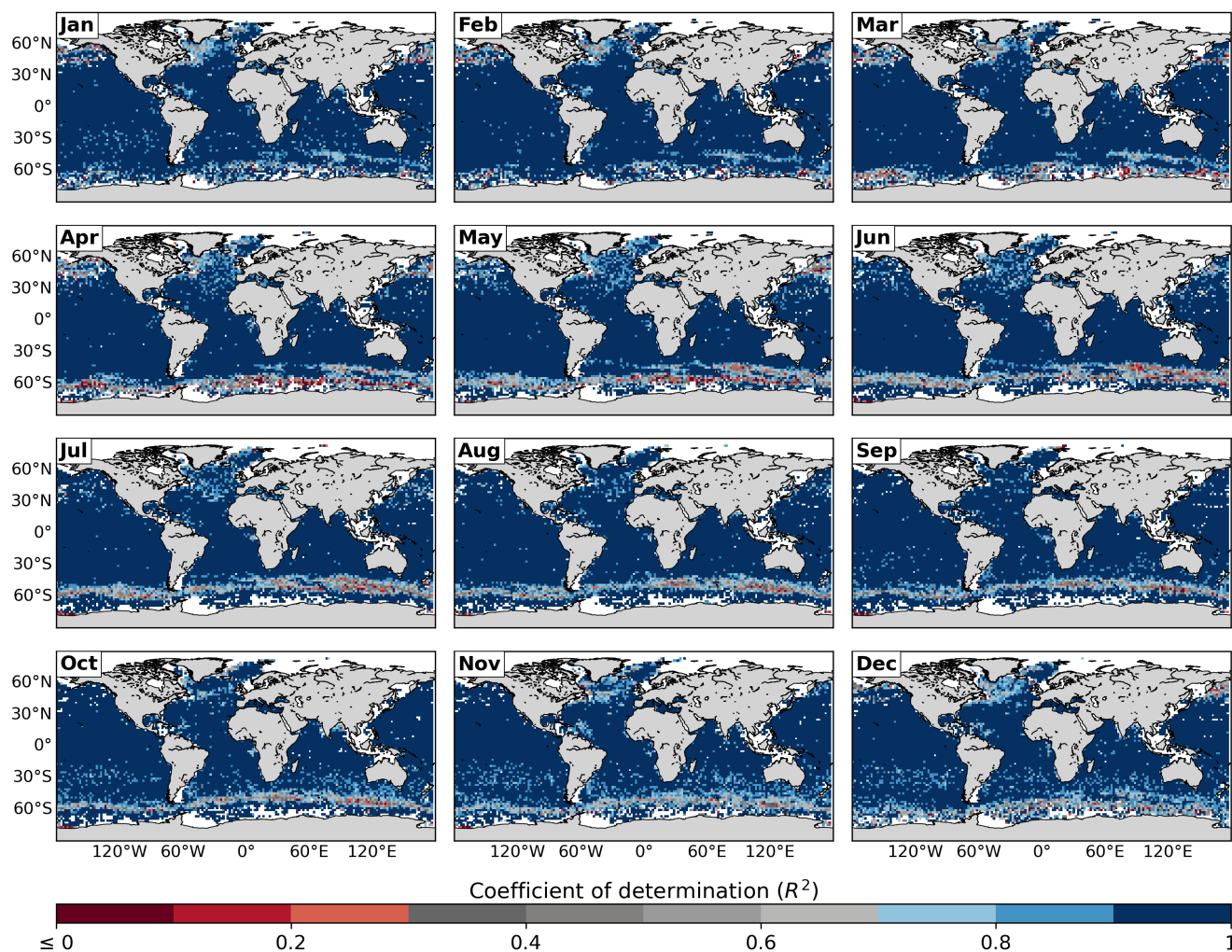


Figure 3. Monthly average of R^2 .

In general terms, the adjustment of the sigmoid function is very good (with $R^2 \geq 0.9$) in low and mid latitudes. However, the cells with red and gray colors should be taken with caution. These present $R^2 < 0.3$ and < 0.7 respectively, which indicates that the adjustment of the sigmoid function was poor or not optimal. The worst adjustments correspond to the core of the Antarctic Circumpolar Current in the Southern Ocean, the North Pacific and the Western North Atlantic. These are regions where the stratification of the water column is dominated by salinity (Figure 2) and/or with strong currents and associated turbulent dynamics. In general terms, in the regions where the adjustment was worse, it was less good in winter months.

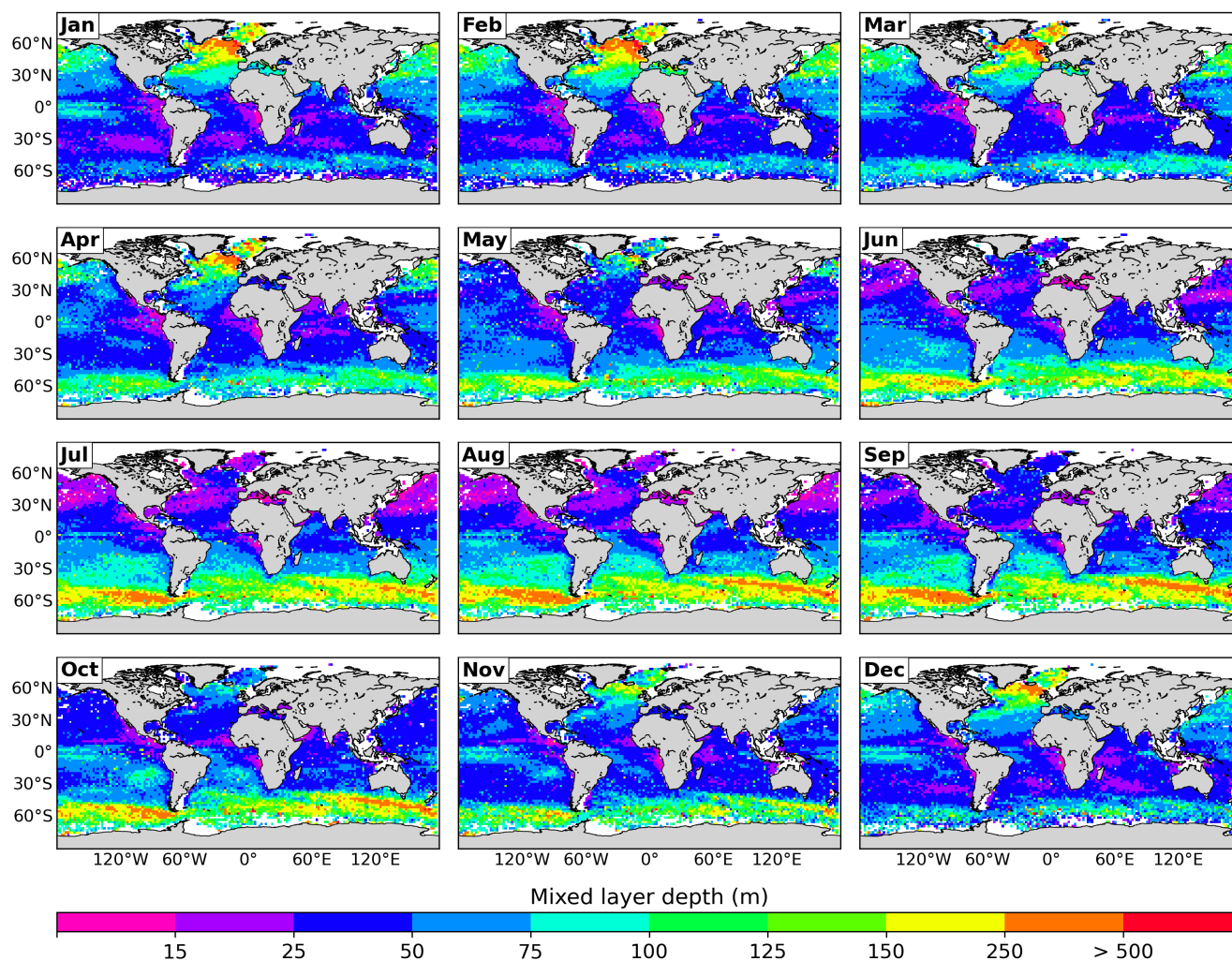


Figure 4. Climatology of the MLD estimated from individual profiles.

4.2 Atlas of the mixed layer depth

The monthly climatology of the MLD computed with the proposed method (Figure 4) reproduces well the spatial patterns and the seasonal variability of the mixed layer as shown in previous studies (e.g., de Boyer Montégut et al., 2004; Holte et al., 2017). It captures the regions with the deepest (northern North Atlantic and Southern Ocean) and the shallowest values (tropical and subtropical areas of both hemispheres) and their magnitudes.

The MLD shows strong seasonality as well as hemispheric asymmetry, mainly in the subtropical and subpolar regions. In the northern hemisphere, in summer months, the mixed layer is generally shallower than 50 m; while in late winter, it reaches climatological mean values over 1000 m in some regions of the North Atlantic basin such as the Labrador Sea, the Nordic Seas.

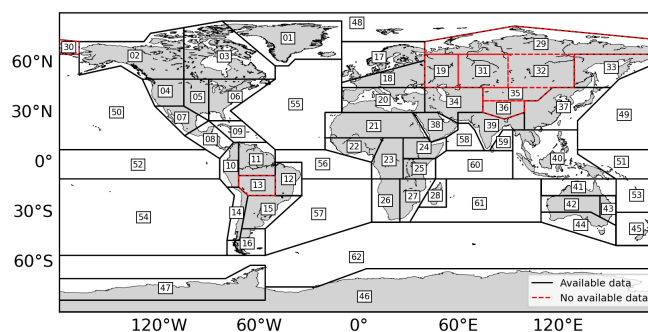


Figure 5. Reference regions of AR6-WGI. The regions used for comparison are those delimited in black.

In the Southern hemisphere, the MLD is generally deeper than in the northern hemisphere, and it is dominated by the signal of the Antarctic Circumpolar Current. The mixed layer in this region varies between 75-100 m depth in summer and around 500 m depth in winter, mainly in the Indian and Pacific basins. In tropical and subtropical latitudes, the MLD is generally very shallow, varying below 15 m in summer up to 150 m depth in winter.

175 In general terms, our climatology agrees with those of Holte et al. (2017), de Boyer Montégut et al. (2004), HT09 and B04 (Figure S1 in the Supplementary information), but there are some differences. For instance, Figure S1 shows how B04 generally overestimates the MLD and has the greatest differences (above 25%) compared to our method and HT09. The HT09 method gives slightly shallower mixed layers than our method in subpolar latitudes, while it overestimates the MLD in tropical and subtropical regions. However, the comparison between our method and HT09 shows no net underestimation
180 or overestimation and the relative difference between both methods is less than $|25\%|$ in most of the ocean. To make a more quantitative comparison, the MLDs computed with the three different methods were averaged within the reference regions of AR6-WGI as described in the methods section (Figure 5).

The red-delimited regions are fully continental regions and were not used for our analysis. The regions with less than 10 averaged values were also excluded. The averages of the MLD computed with each method in each region were plotted for a
185 representative month of each season (Figure 6).

The MLD shows good agreement between the three methods in most regions. In general terms, the method proposed here is in better agreement with HT09, being B04, the one that exhibits the greatest differences. In February and May, the B04 method seems to overestimate the MLD in the regions of Northeast North-America (region 03) and North Europe (region 17) (Figure 6a and b). These are polar regions containing semi enclosed seas in the Northern Hemisphere and mostly in the Arctic-Ocean
190 (region 48). It is likely that these regions exhibit particular dynamics that complicate the detection of the MLD with a threshold based method. One possible explanation is that coastal regions generally are worse sampled, but also, that the computation of the MLD can be complicated by a number of coastal processes such as river discharges or shallow bathymetry among others. Moreover, the traditional delta density criterion of 0.03kgm^{-3} has been suggested to underestimate the MLD in polar regions, as demonstrated in the study by Peralta-Ferriz and Woodgate (2015), where it was found that a better criterion for these regions

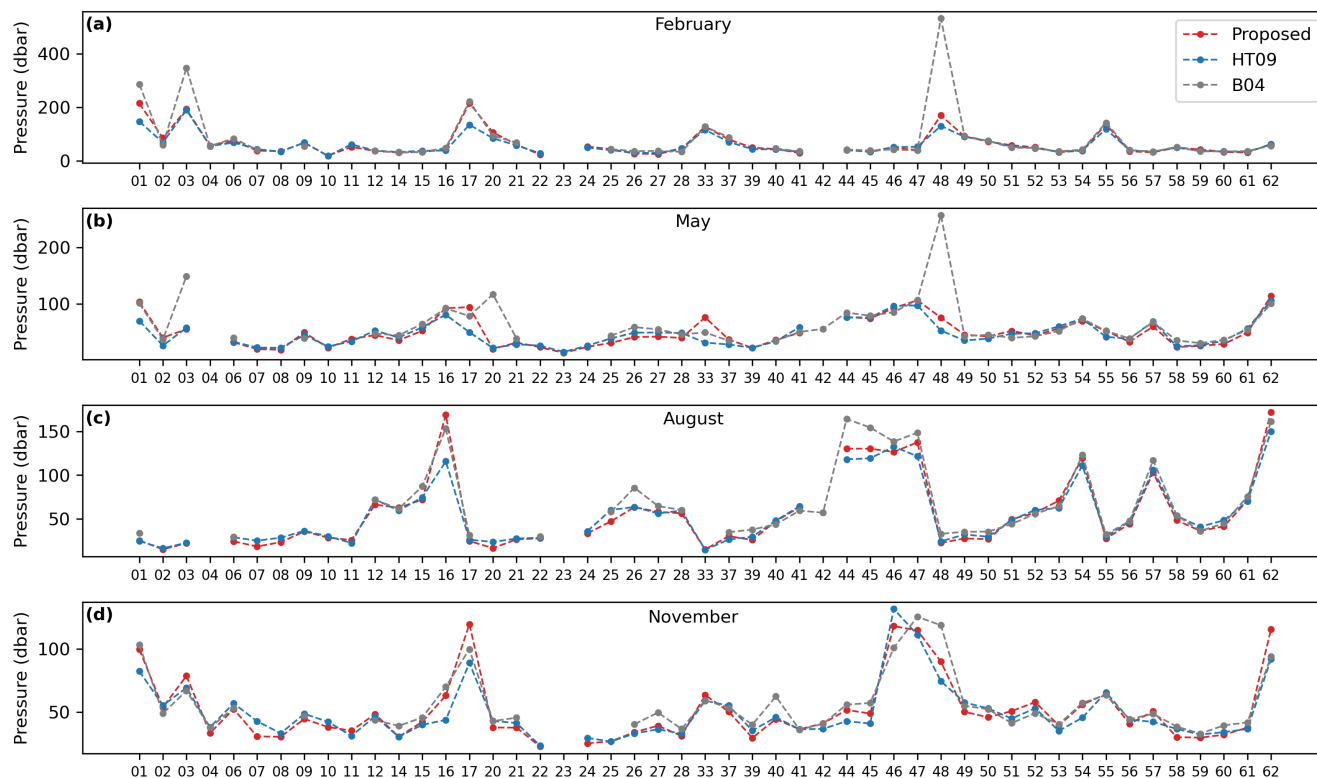


Figure 6. Comparison of methodologies to locate the MLD in (a) February, (b) May, (c) August and (d) November.

195 is 0.1 kg m^{-3} . Interestingly, the agreement between the three methods is also good in the regions where our adjustment was not considered to be good ($R^2 < 0.7$, Figure 3) and in those where salinity dominates the stratification such as region 62 (Figure 2). In other complicated region as the one around Greenland (region 01) there are some differences between the three methods, but the one proposed here either agrees completely with one of the other two (B04 in May and November and HT09 in August) or gives a MLD value that is intermediate regarding the other two methods (as in February). This suggests that although our method is not perfect in these highly dynamical or salinity-dominated regions, it gives results that compare well with other broadly used methods. Moreover, this highlights the possible deficiency of all existing methods in detecting the MLD in these regions.

4.3 Climatology of the maximum thermocline depth and thickness

Once the proposed methodology is validated with the calculation of the MLD, we computed the monthly climatology of the MTD (Figure 7).

As expected, the shape of the MTD follows that of the MLD but the hemispheric asymmetry is not that evident. The subtropical and subpolar regions of the North Atlantic as well as the Southern Ocean exhibit the deepest thermoclines of the

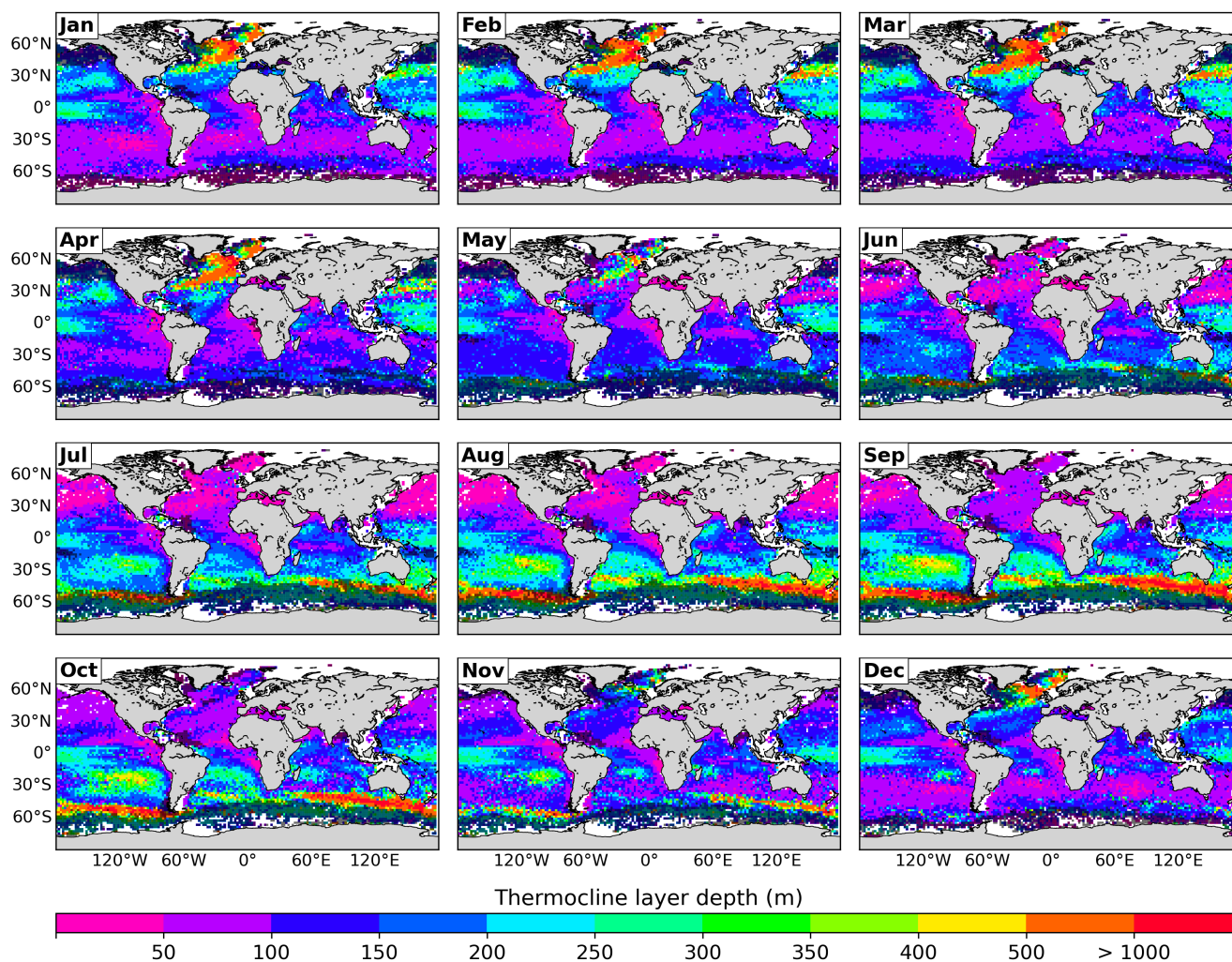


Figure 7. Climatology of the MTD estimated from individual profiles. Shaded cells are those where salinity has a greater contribution to the most stratified point.

ocean. Similarly to the MLD, the deepest thermoclines are found in late winter: March-April in the Northern Hemisphere and September-October in the Southern Ocean. In the northern hemisphere, during the summer the MTD is generally no deeper than 100 m; while in winter, it reaches depths greater than 1000 m in the same regions where the MLD reaches its maximum values (Figure 4), extending to the Gulf Stream in winter and spring months. In the southern hemisphere, the mean climatological MTD values for the summer and winter months are similar to those of the opposite hemisphere.

This climatology shows the same pattern of greater depths in the Antarctic circumpolar current signal that the MLD climatology shows. During the winter and spring months the MTD reaches values deeper than 500 m in the core of the Antarctic Circumpolar Current in the Southern Ocean (reaching more than 1000 m in localized areas). The deeper thermoclines in the

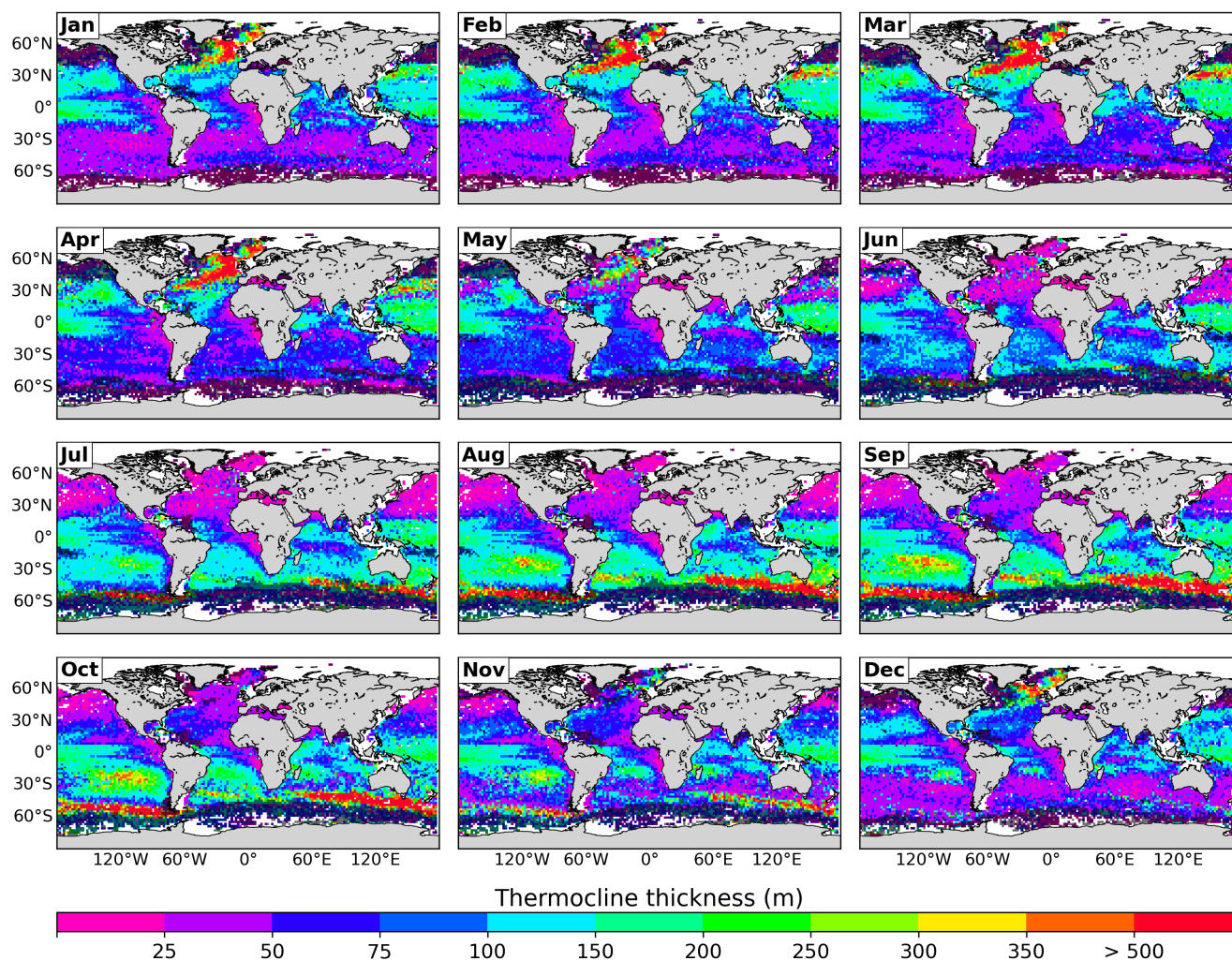


Figure 8. Climatology of the thermocline thickness estimated from individual profiles. Shaded cells are those where salinity has a greater contribution to the most stratified point.

Southern Ocean, in winter, coincide with the seasonality of the zonal band where the inertial horizontal kinetic energy in the mixed layer is larger (Flexas et al., 2019). This energy is injected by the relatively strong winds during these seasons which is also related to the relatively deep MLD (as shown in Figure 4 and therefore of the thermocline).

During summer, the MTD rarely exceeds 50 m depth in the Northern and 75 m in the Southern Hemisphere. In these same regions, the climatologies of the thermocline thickness (Figure 8) presented mainly values below 50m, which suggests that in the regions where the depths of the MLD and the MTD are very shallow, the thickness of the thermocline is reduced.

The thermocline thickness follows a similar pattern than the MLD and the MTD. In the same way as the MLD and the MDT (Figures 4 and 7 respectively), the climatology of the thermocline thickness (Figure 8) presents a marked seasonality



in subtropical and subpolar latitudes. The thickest thermoclines are found in late winter: March-April in the North Atlantic
225 basin and September-October in the Southern Ocean. Away from these regions, the seasonal variability of the thermocline
thickness is low in tropical regions where it varies between 150 and 250 m depending on the region. The thinnest thermoclines
are observed in summer in subtropical/subpolar latitudes of both hemispheres (July -August in the Northern Hemisphere and
January-February in the Southern Hemisphere).

The thermocline thickness follows a similar pattern as the MLD and the MTD. In the same way, the climatology of the
230 thermocline thickness (Figure 8) presents a marked seasonality in subtropical and subpolar latitudes. As expected, the thickest
thermoclines (> 500 m) are found in the regions and periods of lower stratification (i.e., in late winter), March-April in the
North Atlantic basin and September-October in the Southern Ocean, particularly in the region dominated by the Antarctic
Circumpolar Current. Away from these regions, in tropical latitudes, the seasonal variability of the thermocline thickness is
lower, it varies between 150 and 250 m depending on the region. Similarly, the thinnest thermoclines are observed in the
235 most stratified regions, particularly during summer in subtropical/subpolar latitudes of both hemispheres (July-August in the
Northern Hemisphere and January-February in the Southern Hemisphere).

5 Discussion

In this study we have proposed a new method to locate the thermocline. This method is based on the adjustment of a symmetric
sigmoid function that relies on the principle that the thermal structure of the ocean consists of three main layers: the mixing
240 layer, the thermocline and the deep layer of the ocean. Although not all temperature profiles have the shape mentioned above
throughout the ocean, the proposed method relies on the maximum stratification found within the thermocline and the symmetry
of the sigmoid function, to place the diagonal line of the function in the thermocline.

The proposed method, due to the shape of a typical temperature profile in the ocean, also allows us to determine the MLD
and, therefore, we were able to validate it. The climatology of the MLD generated in our study (Figure 4), is in good agreement
245 with those provided by de Boyer Montégut et al. (2004) and Holte et al. (2017). de Boyer Montégut et al. (2004) used a threshold
of 0.03 kg m^{-3} to determine MLD, while Holte et al. (2017) used their two linear function fitting methodology proposed in
Holte and Talley (2009). The three methods reproduce the magnitude, the spatial variability and the seasonal cycle of the MLD
throughout the global ocean in a similar and consistent way for most of the ocean regions. Moreover, in the few regions where
all three methods disagreed, the one proposed here was mostly in line with the results of HT09, while B04 exhibited extreme
250 MLD values.

This can be partly explained by the fact that both methodologies use function adjustments. The study of HT09 bases on the
homogeneity of the MLD to perform a linear function adjustment, in addition to performing another linear function adjust-
ment in the thermocline, while the proposed methodology uses this same MLD feature to determine how deep the sigmoid
function will be adjusted. The regions with the greatest differences between methodologies were found in a small region of the
255 Arctic Ocean and the Labrador Sea (Figure 6a-b). There, the method of B04 strongly differed from our method and that from
HT09. We attribute the overestimation of the B04 method to the fact that staircase stratification have been reported in these



areas (Timmermans et al., 2008; Toole et al., 2011) and during the development of this research, multi-thermoclines and mix thermoclines (Jiang et al., 2017) have been found in these regions.

All the compared studies have used Argo data in their climatologies. However, de Boyer Montégut et al. (2004) being an older study had less data, while Holte et al. (2017) used RTQC data in a $1^\circ \times 1^\circ$ grid (in contrast to the $2^\circ \times 2^\circ$ grid used by us and de Boyer Montégut et al. (2004). This smaller-size grid is not optimal to be used with the amount of DMQC data available, as a large number of cells would contain less than three values for monthly averages. Using RTQC data would increase the amount of data available for our computations. However, Argo recommends using only DMQC for scientific research, since the RTQC tests are automated and may contain bad data, as explained in the manuals (Argo Data Management Team, 2022) and even using the best quality control flag, as shown in Romero et al. (2021), therefore, using this data could cause the erroneous computation of the MLD and MTD.

Using the density to estimate the MLD usually gives good results, since it depends on temperature and salinity, however, the density can show vertical compensation (de Boyer Montégut et al., 2004), therefore, a good alternative to estimate the MLD is to use temperature (Rao et al., 1989). Although the other two methods use density profiles for the calculation of the MLD, this does not give good results with the methodology proposed in this paper. The adjustment of the sigmoid function bases on the typical shape of the temperature profile. In order to calculate the pycnocline with a similar methodology to the one proposed here, it would be necessary to find another function that better fits the density profile. Yamaguchi and Suga (2019) decomposed density stratification into haline and thermal stratification components, and showed that thermal stratification trends contribute more to density stratification trends since the 1960s. Only in regions where salinity is significant (e.g., Subarctic North Pacific, Southern Ocean), salinity stratification trends show contributions to density stratification trends. As shown in Figure 2, in more than 77% of the grid cells the N_T^2 contribution to the maximum stratification of the water column, is equal to or greater than 50%. Therefore our method assumes that in these regions, the maximum N^2 is a good approximation of both, the thermocline, and the pycnocline. In the polar and some subpolar regions of both hemispheres, where salinity is the major contributor to the density gradient (reddish cells in Figure 2) it dominates the stratification. Consequently, in these regions, the thermocline and pycnocline might differ significantly, and our method cannot be used to approximate the pycnocline.

The calculation of the climatologies of the MTD and the thermocline thickness were not compared with the calculation of any other method since no method of calculating these parameters was found that works on a global scale. The latter was reproduced here, and only gave good results with profiles located in tropical latitudes Fiedler (2010), and only gave good results with profiles located in tropical latitudes (Figure S2 in the Supplementary information). As shown in Figure S2, away from the tropics, the calculation of the MLD and MTD with the VRI method does not give good results, in addition to not considering the inverse thermoclines (Figure S2f). For these reasons, the relative contribution of temperature and salinity to the most stratified point of the water column and the performance in fitting the sigmoid function were used to validate the method.

Our method showed generally good performance in the adjustment of the sigmoid function to the temperature profiles (expressed by the R^2) with the exception of a few regions: the North Pacific Ocean, the northern North Atlantic Ocean, the Arctic Ocean and the core of the Antarctic Circumpolar Current in the Southern Ocean. While the interpretation of the MLD and the MTD in these regions has to be made with caution, it is noteworthy that the values of R^2 are not a direct indicator



of the precision of the method to calculate the MLD and the MTD. Rather, this index shows the goodness of the sigmoid function fit to the temperature profile. Precisely, in the most problematic regions mentioned above, R^2 is lower than 0.7 in some months (Figure 3). However, the three methods used for the MLD calculation give very similar values (Figure 6) even in
295 these regions. This suggests that it is not a particular shortcoming of our adjustment. Previous studies such as those by Peralta-Ferriz and Woodgate (2015) and Pellichero et al. (2016) have shown the variability in the calculation of the MLD in these regions depending on the methods and thresholds used. This has evidenced that these are complex, highly dynamical regions (i.e., turbulent regions with important eddy activity), where the estimation of the MLD in a reliable way is a complicated task. In this sense, it has been suggested that in the Southern Ocean the MLD calculation is less accurate than in regions at lower
300 latitudes where the water column is strictly temperature stratified (Dong et al., 2008). The low values of R^2 shown in Figure 3 are due to the abrupt changes in temperature in the profiles measured in these regions. These abrupt changes might be related to well known processes taking place in certain regions of the ocean as: (i) double-diffusive staircase stratification in the Arctic (Timmermans et al., 2008; Toole et al., 2011), and (ii) to the temperature inversions due to the influence of salinity that present different vertical structures in the Southern Ocean (Dong et al., 2008).

305 The results of our adjustment also evidence the regions of the ocean where the water column exhibits a typical vertical thermal structure in three layers and the regions where, due to their dynamics, the structure of the water column cannot be divided in these three layers. The efficiency provided by the proposed method for the calculation of the MLD and the MTD, allows to perform local to global studies. For example, in the context of ocean warming, the differences of these layers could be compared temporarily to analyze the changes of the water column, detecting areas of the ocean where the thermocline has
310 changed its depth or thickness over time, and therefore to be a parameter of the potential effects on the pelagic ecosystem and socio-economic repercussions.

6 Conclusions

In this study, we present a methodology to locate the minimum and maximum depth of the thermocline and its thickness by adjusting the sigmoid function to the temperature profiles in the global ocean. This methodology can be applied to both
315 global and local studies in those areas of the ocean where the water column can be divided into three layers according to its thermal structure. Our methodology gave good results in its validation against other two broadly used methodologies in the global ocean. The MLD computed with the three methods showed a high correlation, even in regions where the coefficient of determination suggested a poor adjustment. This suggests that it is not a particular shortcoming of our method, but rather a general difficulty in determining the limits of the three typical oceanic thermal layers in highly turbulent regions.

320 *Code availability.* The methodology presented in this study was developed in Python 3.7 and is licensed under a Creative Commons Attribution 4.0 International License. The source code is available at <https://doi.org/10.5281/zenodo.6985561> (Romero et al., 2022). The latest package version is v1.0.1.



Data availability. These data were collected and made freely available by the International Argo Program and the national programs that contribute to it (<https://argo.ucsd.edu>, last access: January 2022; <https://www.ocean-ops.org>, last access: January 2022). The Argo Program
325 is part of the Global Ocean Observing System. The data used belongs to the snapshot of January 2022 (Argo, 2022b).

Author contributions. ER developed the methodology described in this work and carried out the analyses. All co-authors contributed to the conceptualization and design of the study, the interpretation of the results, and the preparation of the article.

Competing interests. The authors declare that they have no conflict of interest.

Acknowledgements. We are grateful to CONACYT for granting scholarship no. 780669 to Emmanuel Romero. We appreciate that these
330 data were collected and made freely available by the International Argo Program and the national programs that contribute to it (<https://argo.ucsd.edu>, last access: January 2022; <https://www.ocean-ops.org>, last access: January 2022). The Argo Program is part of the Global Ocean Observing System. We also thank the Centro Interdisciplinario de Ciencias Marinas (CICIMAR) for their institutional support. We also acknowledge the critical comments from the reviewers.



References

- 335 Argo: Argo, <https://argo.ucsd.edu/>, 2022a.
Argo: Argo float data and metadata from Global Data Assembly Centre (Argo GDAC), <https://doi.org/10.17882/42182>, 2022b.
Argo Data Management Team: Argo user's manual, <https://doi.org/10.13155/29825>, 2022.
- Chu, P. C. and Fan, C.: Exponential leap-forward gradient scheme for determining the isothermal layer depth from profile data, *Journal of Oceanography*, 73, 503–526, <https://doi.org/10.1007/s10872-017-0418-0>, 2017.
- 340 Chu, P. C. and Fan, C.: Global ocean synoptic thermocline gradient, isothermal-layer depth, and other upper ocean parameters, *Scientific Data*, 6, 119, <https://doi.org/10.1038/s41597-019-0125-3>, 2019.
- de Boyer Montégut, C., Madec, G., Fischer, A. S., Lazar, A., and Iudicone, D.: Mixed layer depth over the global ocean: An examination of profile data and a profile-based climatology, *Journal of Geophysical Research: Oceans*, 109, <https://doi.org/10.1029/2004JC002378>, 2004.
- Dong, S., Sprintall, J., Gille, S. T., and Talley, L.: Southern Ocean mixed-layer depth from Argo float profiles, *Journal of Geophysical*
345 *Research: Oceans*, 113, <https://doi.org/10.1029/2006JC004051>, 2008.
- Fiedler, P. C.: Comparison of objective descriptions of the thermocline, *Limnology and Oceanography: Methods*, 8, 313–325, <https://doi.org/10.4319/lom.2010.8.313>, 2010.
- Flexas, M. M., Thompson, A. F., Torres, H. S., Klein, P., Farrar, J. T., Zhang, H., and Menemenlis, D.: Global Estimates of the Energy Transfer From the Wind to the Ocean, With Emphasis on Near-Inertial Oscillations, *Journal of Geophysical Research: Oceans*, 124, 5723–5746,
350 <https://doi.org/10.1029/2018JC014453>, 2019.
- Gévaudan, M., Jouanno, J., Durand, F., Morvan, G., Renault, L., and Samson, G.: Influence of ocean salinity stratification on the tropical Atlantic Ocean surface, *Climate Dynamics*, 57, 321–340, <https://doi.org/10.1007/s00382-021-05713-z>, 2021.
- Harper, S.: Thermocline ventilation and pathways of tropical–subtropical water mass exchange, *Tellus A: Dynamic Meteorology and Oceanography*, 52, 330–345, <https://doi.org/10.3402/tellusa.v52i3.12269>, 2000.
- 355 Holte, J. and Talley, L.: A New Algorithm for Finding Mixed Layer Depths with Applications to Argo Data and Subantarctic Mode Water Formation, *Journal of Atmospheric and Oceanic Technology*, 26, 1920–1939, <https://doi.org/10.1175/2009JTECHO543.1>, 2009.
- Holte, J., Talley, L. D., Gilson, J., and Roemmich, D.: An Argo mixed layer climatology and database, *Geophysical Research Letters*, 44, 5618–5626, <https://doi.org/10.1002/2017GL073426>, 2017.
- Iturbide, M., Gutiérrez, J. M., Alves, L. M., Bedia, J., Cerezo-Mota, R., Cimadevilla, E., Cofiño, A. S., Luca, A. D., Faria, S. H., Gorodetskaya, I. V., Hauser, M., Herrera, S., Hennessy, K., Hewitt, H. T., Jones, R. G., Krakovska, S., Manzanar, R., Martínez-Castro, D., Narisma, G. T., Nurhati, I. S., Pinto, I., Seneviratne, S. I., van den Hurk, B., and Vera, C. S.: An update of IPCC climate reference regions for subcontinental analysis of climate model data: definition and aggregated datasets, *Earth System Science Data*, 12, 2959–2970, <https://doi.org/10.5194/essd-12-2959-2020>, 2020.
- 360 Jiang, B., Wu, X., and Ding, J.: Comparison of the calculation methods of the thermocline depth of the South China Sea, *Mar. Sci. Bull.*, 35, 64–73, 2016.
- Jiang, Y., Gou, Y., Zhang, T., Wang, K., and Hu, C.: A Machine Learning Approach to Argo Data Analysis in a Thermocline, *Sensors*, 17, <https://doi.org/10.3390/s17102225>, 2017.
- Landerer, F. W., Jungclauss, J. H., and Marotzke, J.: Regional Dynamic and Steric Sea Level Change in Response to the IPCC-A1B Scenario, *Journal of Physical Oceanography*, 37, 296–312, <https://doi.org/10.1175/JPO3013.1>, 2007.



- 370 Li, G., Cheng, L., Zhu, J., Trenberth, K. E., Mann, M. E., and Abraham, J. P.: Increasing ocean stratification over the past half-century, *Nature Climate Change*, 10, 1116–1123, <https://doi.org/10.1038/s41558-020-00918-2>, 2020.
- Li, Y., Han, W., Ravichandran, M., Wang, W., Shinoda, T., and Lee, T.: Bay of Bengal salinity stratification and Indian summer monsoon intraseasonal oscillation: 1. Intraseasonal variability and causes, *Journal of Geophysical Research: Oceans*, 122, 4291–4311, <https://doi.org/https://doi.org/10.1002/2017JC012691>, <https://doi.org/10.1002/2017JC012691>, 2017.
- 375 Luo, Y., Rothstein, L. M., and Zhang, R.-H.: Response of Pacific subtropical-tropical thermocline water pathways and transports to global warming, *Geophysical Research Letters*, 36, <https://doi.org/10.1029/2008GL036705>, 2009.
- McDougall, T. and Barker, P.: Getting started with TEOS-10 and the Gibbs Seawater (GSW) Oceanographic Toolbox, SCOR/IAPSO WG127, 2011.
- Overland, J. E. and Wang, M.: Future climate of the north Pacific Ocean, *Eos, Transactions American Geophysical Union*, 88, 178–182, <https://doi.org/10.1029/2007EO160003>, 2007.
- 380 Pellichero, V., Sallée, J.-B., Schmidtko, S., Roquet, F., and Charrassin, J.-B.: The ocean mixed layer under Southern Ocean sea-ice: Seasonal cycle and forcing, *Journal of Geophysical Research: Oceans*, 122, 1608–1633, <https://doi.org/10.1002/2016JC011970>, 2016.
- Peralta-Ferriz, C. and Woodgate, R. A.: Seasonal and interannual variability of pan-Arctic surface mixed layer properties from 1979 to 2012 from hydrographic data, and the dominance of stratification for multiyear mixed layer depth shoaling, *Progress in Oceanography*, 134, 19–53, <https://doi.org/10.1016/j.pocean.2014.12.005>, 2015.
- 385 Portela, E., Kolodziejczyk, N., Vic, C., and Thierry, V.: Physical Mechanisms Driving Oxygen Subduction in the Global Ocean, *Geophysical Research Letters*, 47, e2020GL089040, <https://doi.org/https://doi.org/10.1029/2020GL089040>, 2020.
- Rao, R. R., Molinari, R. L., and Festa, J. F.: Evolution of the climatological near-surface thermal structure of the tropical Indian Ocean: 1. Description of mean monthly mixed layer depth, and sea surface temperature, surface current, and surface meteorological fields, *Journal of Geophysical Research: Oceans*, 94, 10 801–10 815, <https://doi.org/10.1029/JC094iC08p10801>, 1989.
- 390 Romero, E., Tenorio-Fernandez, L., Castro, I., and Castro, M.: Filtering method based on cluster analysis to avoid salinity drifts and recover Argo data in less time, *Ocean Science*, 17, 1273–1284, <https://doi.org/10.5194/os-17-1273-2021>, 2021.
- Romero, E., Tenorio-Fernandez, L., Portela, E., Montes-Aréchiga, J., and Sánchez-Velasco, L.: `romeroqe/mld-mtd: MLD MTD`, <https://doi.org/10.5281/zenodo.6985561>, 2022.
- 395 Ruvalcaba-Aroche, E. D., Sánchez-Velasco, L., Beier, E., Barton, E. D., Godínez, V. M., Gómez-Gutiérrez, J., and Martínez-Rincón, R. O.: Ommastrephid squid paralarvae potential nursery habitat in the tropical-subtropical convergence off Mexico, *Progress in Oceanography*, 202, 102 762, <https://doi.org/10.1016/j.pocean.2022.102762>, 2022.
- Sallée, J.-B., Matear, R. J., Rintoul, S. R., and Lenton, A.: Localized subduction of anthropogenic carbon dioxide in the Southern Hemisphere oceans, *Nature Geoscience*, 5, 579–584, <https://doi.org/10.1038/ngeo1523>, 2012.
- 400 Sallée, J.-B., Pellichero, V., Akhoudas, C., Pauthenet, E., Vignes, L., Schmidtko, S., Garabato, A. N., Sutherland, P., and Kuusela, M.: Summertime increases in upper-ocean stratification and mixed-layer depth, *Nature*, 591, 592–598, <https://doi.org/10.1038/s41586-021-03303-x>, 2021.
- Southward, A. J. and Barrett, R. L.: Observations on the vertical distribution of zooplankton, including post-larval teleosts, off Plymouth in the presence of a thermocline and a chlorophyll-dense layer, *Journal of Plankton Research*, 5, 599–618, <https://doi.org/10.1093/plankt/5.4.599>, 1983.
- 405 Sprintall, J. and Cronin, M. F.: Upper Ocean Vertical Structure, <https://doi.org/10.1006/rwos.2001.0149>, 2001.



- Timmermans, M.-L., Toole, J., Krishfield, R., and Winsor, P.: Ice-Tethered Profiler observations of the double-diffusive staircase in the Canada Basin thermocline, *Journal of Geophysical Research: Oceans*, 113, <https://doi.org/10.1029/2008JC004829>, 2008.
- Toole, J. M., Krishfield, R. A., Timmermans, M.-L., and Proshutinsky, A.: The ice-tethered profiler: Argo of the Arctic, *Oceanography*, 24, 126–135, <http://www.jstor.org/stable/24861307>, 2011.
- 410 Vecchi, G. and Soden, B.: Global Warming and the Weakening of the Tropical Circulation, *Journal of Climate - J CLIMATE*, 20, <https://doi.org/10.1175/JCLI4258.1>, 2007.
- Webb, P.: *Introduction to Oceanography*, Roger Williams University, <http://rwu.pressbooks.pub/webboceanography>, 2021.
- Yamaguchi, R. and Suga, T.: Trend and Variability in Global Upper-Ocean Stratification Since the 1960s, *Journal of Geophysical Research: Oceans*, 124, 8933–8948, <https://doi.org/10.1029/2019JC015439>, 2019.
- 415 Yang, H. and Wang, F.: Revisiting the Thermocline Depth in the Equatorial Pacific, *Journal of Climate*, 22, 3856–3863, <https://doi.org/10.1175/2009JCLI2836.1>, 2009.
- Zelle, H., Appeldoorn, G., Burgers, G., and van Oldenborgh, G. J.: The Relationship between Sea Surface Temperature and Thermocline Depth in the Eastern Equatorial Pacific, *Journal of Physical Oceanography*, 34, 643–655, <https://doi.org/10.1175/2523.1>, 2004.